Nonadiabatic interaction of a propagating wave packet with localized parametric pumping

G. A. Melkov, A. A. Serga, V. S. Tiberkevich, and Yu. V. Kobljanskij
Radiophysical Faculty, National Taras Shevchenko University of Kiev, Kiev, Ukraine

A. N. Slavin
Department of Physics, Oakland University, Rochester, Michigan 48309

(Received 29 January 2001; published 23 May 2001)

The interaction of a propagating wave packet (carrier frequency ω, wave number k) with nonadiabatic parametric pumping, localized in a region of size the order of the carrier wavelength $L \sim \lambda = 2\pi/k$, is studied experimentally in a system of dipolar spin waves in a ferrite film. It is shown that the three-wave parametric interaction $\omega + \omega' = \omega_p$ leads to the formation of both contrapropagating ($k' = -k$) and copropagating ($k' = k$) idle wave packets of carrier frequency ω'. A system of equations derived for the packet envelopes gives a quantitative description of the observed random modulation of the output signal caused by the interference of the input and copropagating idle wave packets.

DOI: 10.1103/PhysRevE.63.066607 PACS number(s): 75.30.Ds, 76.50.+g, 85.70.Ge

Parametric interaction of a propagating wave with electromagnetic pumping in a nonlinear medium always occurs in a limited spatial region of length L (if we consider a one-dimensional case). Usually, the interaction satisfies the adiabatic condition [1,2]

$$kL \gg 1, \tag{1}$$

which means that the length L of the pumping localization region is large compared to the wavelength $\lambda = 2\pi/k$ of the propagating wave of wave number k. If the adiabatic condition (1) is fulfilled, the interaction with pumping results in a parametric coupling between the signal wave (frequency ω, wave number k) and the idle wave (frequency ω', wave number k') satisfying the conservation laws

$$\omega + \omega' = \omega_p, \tag{2a}$$

$$k + k' = k_p, \tag{2b}$$

where ω_p and k_p are the frequency and wave number of the parametric pumping. Here and below we shall consider only the case of the one-dimensional (waves propagate along the z axis) three-wave (first order) parametric interaction (2).

The parametric interaction (2) of two spectrally narrow (quasimonochromatic) wave packets with adiabatic pumping (1) is usually described by a system of reduced equations for the envelope amplitudes $a_k(t,z)$ of interacting wave packets [3,4]. This system has been used successfully in different branches of physics, such as nonlinear optics [5], plasma physics [6], and magnetism [7].

It turns out that the character of the wave instability under the influence of parametric pumping, as well as the directions of propagation of the interacting wave packets, depend critically on the relative values of the wave numbers k, k', and k_p. If $k_p \simeq 2k \simeq 2k'$ (and the pumping is a propagating wave, as is usually the case in nonlinear optics [5]), a *convective* instabilty of two copropagating wave packets ($k' = k$) moving in the same direction as the pumping wave occurs [8]. In this case the system of reduced equations has the form [4]

$$\left(\frac{\partial}{\partial t} + v\frac{\partial}{\partial z} + \Gamma\right) a_k(t,z) = V_{k,k} b_{2k}(t,z) a_k^*(t,z), \tag{3a}$$

$$\left(\frac{\partial}{\partial t} + v\frac{\partial}{\partial z} + \Gamma\right) a_k^*(t,z) = V_{k,k}^* b_{2k}^*(t,z) a_k(t,z), \tag{3b}$$

where v and Γ are the velocity and dissipation of the parametric wave packet $a_k(t,z)$ having carrier wave vector k; $V_{k,k'}$ is the coupling coefficient between the parametric waves and the pumping; $b_{2k}(t,z)$ is the pumping amplitude, which in the simplest case is the slowly varying complex amplitude of the electric or magnetic field of the pumping wave having carrier wave number $2k$.

On the other hand, if the pumping is quasihomogeneous $k, k' \gg k_p \simeq 0$, as is usually the case for parallel pumping of plane spin waves in ferromagnets [7,9], an *absolute* instability of contrapropagating waves ($k' = -k$) is observed [8]. To describe the parametric coupling between these contrapropagating waves the system of reduced equations can be written in the form

$$\left(\frac{\partial}{\partial t} + v\frac{\partial}{\partial z} + \Gamma\right) a_k(t,z) = V_{k,-k} b_0(t,z) a_{-k}^*(t,z), \tag{4a}$$

$$\left(\frac{\partial}{\partial t} - v\frac{\partial}{\partial z} + \Gamma\right) a_{-k}^*(t,z) = V_{k,-k}^* b_0^*(t,z) a_k(t,z). \tag{4b}$$

In this case the pumping is a localized, nonpropagating ($k_p = 0$) electromagnetic field.

In this paper we show that in the case when a signal wave packet of carrier wave number k interacts parametrically with nonadiabatic (or strongly localized) pumping

$$kL \leqslant 1, \tag{5}$$

the excitation of both copropagating ($k' = k$) and contrapropagating ($k' = -k$) idle wave packets is possible simultaneously. This process becomes possible due to the ''smearing'' of the wave number of the strongly localized pumping in the interval $\Delta k_p \simeq 2\pi/L$ near the pumping carrier wave

 ©2001 The American Physical Society

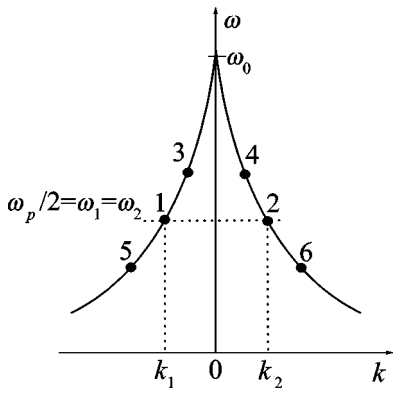

FIG. 1. Spectrum ω_k of the lowest mode of a BVMSW in a tangentially magnetized magnetic film.

number k_{p0}. If the length L of the pumping localization region is such that $2\pi/L \geqslant 2k$, then the wave number spectrum of the localized pumping contains not only $k_p=0$ but also components with $k_p=2k$. Thus, independently of whether the input pumping signal is an oscillation with carrier wave number $k_{p0}\simeq 0$, or a propagating wave with $k_{p0}\simeq 2k$, the wave number spectrum of the strongly localized (nonadiabatic) pumping will contain both components $k_p=0$ and $k_p=2k$.

It should be noted that, in spite of the pumping smearing in k space, the signal and idle wave packets remain spectrally narrow in the frequency space (similar to the well-known case of adiabatic pumping) due to the strong frequency selectivity of the parametric interaction. This important property of a parametric interaction allows us to derive an approximate system of reduced equations for the envelopes of interacting wave packets even in the nonadiabatic case. This system takes into account the simultaneous existence of co- and contrapropagating idle wave packets and presents a direct generalization of Eqs. (3) and (4), traditionally used to describe parametric interaction with pumping in the adiabatic case. Analysis of this generalized system yields a value of the parametric instability threshold $P_{p\,th}$ that is smaller than in the adiabatic case.

The generalized system of reduced equations derived below gives a quantitative description of the experimental results obtained in the case of nonadiabatic pumping of backward volume magnetostatic waves (BVMSW's) (or dipolar spin waves) [10], propagating along the direction of a bias magnetic field H_0 in a tangentially magnetized yttrium iron garnet (YIG) film.

The experimental realization of nonadiabatic pumping is difficult to achieve in optics, as the pumping localization length ($L \leqslant \lambda$) there must be below 1 μm. It is, however, easy to achieve nonadiabatic pumping conditions for dipolar spin waves in ferrite films using strip-line pumping transducers [11,12]. Below we shall discuss in detail nonadiabatic pumping in a system of dipolar spin waves in magnetic films.

The spectrum ω_k of the lowest mode of the BVMSW in a tangentially magnetized magnetic film is presented in Fig. 1. This spectrum is symmetric $\omega_k=\omega_{-k}$, and has an upper boundary of $\omega_0=\gamma\sqrt{H_0(H_0+4\pi M_0)}$, where $\gamma/2\pi=2.8$ MHz/Oe is the gyromagnetic ratio, H_0 is the bias magnetic field, and M_0 is the film saturation magnetization [10]. By choosing the excitation frequency (when the value of H_0 is fixed) it is easy to change the wave number k of the signal wave packet from several to several hundreds of inverse centimeters.

In the following we assume that the signal BVMSW of the frequency ω_k is propagating along the axis z in a film of length l and is interacting with homogeneous parametric pumping of frequency ω_p localized in a spatial region of length L. The equation for the amplitude c_k of this wave can be written in the form [13]

$$\frac{\partial c_k}{\partial t}+i\omega_k c_k+\Gamma_k c_k=\sum_{k'=-\infty}^{\infty}\frac{L}{l}V_{kk'}h_{k+k'}\exp(-i\omega_p t)c_{k'}^{*}, \tag{6}$$

where $\Gamma_k=\gamma\Delta H$ is the wave dissipation parameter, ΔH is the half-linewidth of ferromagnetic resonance in the film, $V_{kk'}$ is given by [13]

$$V_{kk'}=\frac{\omega_k\omega_{k'}-(\gamma H_0)^2}{4H_0\sqrt{\omega_k\omega_{k'}}}, \tag{7}$$

and h_k is the kth Fourier harmonic of the spatially localized pumping field $h_p(z)$,

$$h_k=\frac{1}{L}\int_0^l h_p(z)\exp(-ikz)dz. \tag{8}$$

It is worth noting that the pumping here is not an eigenexcitation of the spin system (i.e., not a dipolar spin wave), and does not obey the dispersion law for BVMSW's. Thus, we can independently change the spectral width of pumping in the frequency space by choosing the duration τ_p of the pumping pulse, and the spectral width of pumping in the wave number space by choosing the spatial width of the pumping localization region L.

First of all, we shall give a qualitative picture of the action of nonadiabatic pumping. Equation (6) describes parametric coupling of waves having wave numbers k and k'. In the case of infinitely extended $L\to\infty$ (purely homogeneous) pumping the coupling of propagating waves with pumping does not vanish only for the waves with wave numbers $k=k_1$ and $k'=k_2=-k_1$, and frequencies $\omega=\omega'=\omega_p/2$, denoted by the numbers 1 and 2 in Fig. 1.

When the pumping field is localized in a region of finite length L, this field can be represented in k space as the sum of monochromatic pumping waves having amplitudes h_k, and wave numbers mostly in the interval $0<|k_p|<2\pi/L$. Thus, the parametric coupling in Eq. (6) becomes possible for any pair of waves with wave numbers k and k' such that $|k+k'|\leqslant 2\pi/L$. With the decrease of L the number of interacting waves increases, and their frequencies, while still satisfying the condition (2a), could be different from $\omega_p/2$ (see, e.g., the waves denoted by the numbers 3, 6 and 4, 5 in Fig. 1 for which $|k_{3,5}+k_{6,4}|\leqslant 2\pi/L$). Note, however, that as long as the condition (1) is fulfilled, these parametrically interacting wave pairs remain contrapropagating.

Finally, when the pumping localization region is so small that $2\pi/L > 2k$ and the adiabatic condition (1) is broken, the interaction of copropagating waves (e.g., waves 3, 5 and 4, 6 in Fig. 1) becomes possible as well. Thus, the simultaneous parametric coupling of both contrapropagating and copropagating waves is possible only when the pumping becomes nonadiabatic.

To obtain a quantitative confirmation of the qualitative analysis presented above of the influence of nonadiabatic pumping we performed numerical calculations in wave number space using the model Eq. (6) for the Fourier amplitudes c_k of the input signal. The central pumping frequency was chosen to be $\omega_p = 2\pi \times 9346$ MHz. The pumping was assumed to be a rectangular temporal radio pulse of duration $\tau_p = 30$ ns localized along the axis z in a region of length $L = 0.1$ mm in a film of length $l = 10$ mm. The bias magnetic field, determining the upper boundary ω_0 in the BVMSW spectrum, was chosen to be $H_0 = 1015$ Oe, while the saturation magnetization $4\pi M_0 = 1750$ Oe and the relaxation parameter $\Gamma_k = 3.5 \times 10^6$ s^{-1} ($\Delta H_k = 0.2$ Oe) were typical for high-quality YIG films [11–14]. The input signal was chosen in the form of a temporal radio pulse having a bell-shaped envelope $[c(t) = \cosh^{-1}(1.76t/\tau_s)]$ of duration $\tau_s = 20$ ns, and carrier frequency $\omega_s = \omega_p/2 + 2\pi \times 50$ MHz $= 2\pi \times 4723$ MHz (see point 3 in Fig. 1). The carrier signal wave number was $k_s = 100$ cm^{-1} ($\lambda_s \simeq 0.6$ mm), so the condition of nonadiabatic interaction (5) was fullfilled. In our calculations we took into account 300 waves with wave numbers k, k' in the interval from -300 cm^{-1} to $+300$ cm^{-1}, and the coupling coefficient $V_{kk'}$ was calculated using Eq. (7).

The power spectra $|c_k(\Delta\omega)|^2$ (where $\Delta\omega = \omega - \omega_p/2$) of the signal transmitted ($k > 0$) through the region of nonadiabatic pumping are presented in Fig. 2. They were calculated from Eq. (6) for different values of the pumping power ($P_p \sim |h_p|^2$).

In the absence of pumping [Fig. 2(a), $P_p = 0$] the output signal is identical to the input signal and in the frequency space yields a spectrally narrow wave packet with carrier frequency $\omega_s = \omega_p/2 + 2\pi \times 50$ MHz, corresponding to point 3 in Fig. 1.

When the pumping power is nonzero but less than the threshold of parametric excitation of BVMSW's by localized nonadiabatic pumping $P_{p\,th}$ [defined below by Eq. (13)], an additional wave packet with the central frequency $\omega_i = \omega_p - \omega_s = \omega_p/2 - 2\pi \times 50$ MHz appears in the output signal. This case for $P_p = 0.8 P_{p\,th}$ is shown in Fig. 2(b). This new wave packet corresponds to the point 5 in Fig. 1 and is not present in the case of adiabatic ($kL \gg 1$) pumping. The reversed signal ($k < 0$, not shown in Fig. 2), created in the interaction of the input signal with pumping, also consists of two separate partial wave packets corresponding to the points 4 and 6 in Fig. 1. Thus, it can be seen that below the threshold of parametric excitation the presence of strongly localizated (nonadiabatic) pumping leads to the parametric interaction of not two, as in the adiabatic case, but four wave packets: one signal and three idle wave packets shown in Fig. 1 by the numbers 3 and 4, 5, 6, respectively.

When the pumping power exceeds the threshold of

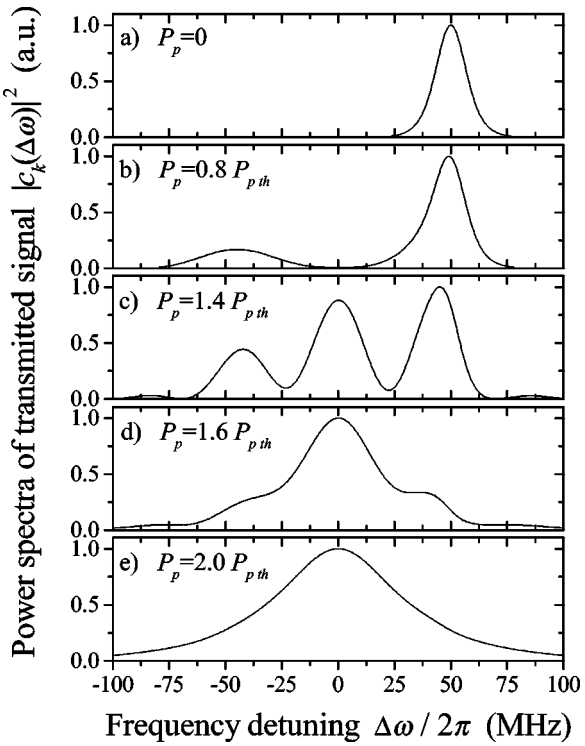

FIG. 2. Spectra of the signal transmitted through the region of nonadiabatic pumping for different values of the pumping power P_p. $P_{p\,th}$ is threshold pumping power for parametric excitation of BVMSW's.

BVMSW excitation $P_{p\,th}$, a new spectral packet having central frequency exactly equal to $\omega_p/2$ appears in the transmitted [Figs. 2(c), 2(d), and 2(e)] and reversed output signals (points 1 and 2 in Fig. 1). With increase of pumping power all the partial spectral packets broaden, begin to overlap, and, finally, for $P_p = 2P_{p\,th}$, form a single spectral packet with the central frequency $\omega_p/2$ [see Fig. 2(e)]. In the case when the input signal is centered around $\omega_p/2$ the picture simplifies significantly as only one spectral packet [similar to the packet in Fig. 2(e)] exists at all levels of the pumping power.

It is well known from the theory of parametric interaction [15] that the phases of all waves at the signal frequency $\omega = \omega_s$ coincide with the phase of the input signal ϕ_s (see points 3 and 4 in Fig. 1). In contrast, the phases ϕ_i of waves at the idle frequency $\omega' = \omega_i = \omega_p - \omega_s$ (points 5 and 6 in Fig. 1) are also dependent on the phase of the pumping ϕ_p: $\phi_i = \phi_p - \phi_s + \pi/2$. These phase relations do not affect the amplitudes of transmitted and reversed signals in any way, if the partial wave packets in these signals do not overlap [see e.g., Fig. 2(b)], although in the pulsed regime the phase difference between these packets is random due to the randomness of the phases of both signal and pumping.

On the other hand, if the partial wave packets do overlap, then in the overlap region each spectral component is an algebraic sum of spectral components from different partial wave packets, and the phase differences between packets become very important. Thus, the amplitudes of the spectral components in the overlap region will vary from the maximum value A_{max}, corresponding to constructive interference

between components from different partial packets, to the minimum value A_{min}, corresponding to destructive interference. This interference between partial wave packets in the pulsed regime will result in random modulation of the output signal (both transmitted and reversed) with the modulation coefficient (in power) given by

$$K_{mod}=\frac{A_{max}^2-A_{min}^2}{A_{max}^2+A_{min}^2}. \tag{9}$$

Analysis of the calculated signal spectra Fig. 2 shows that even in the case of nonadiabatic parametric pumping transmitted wave packets remain spectrally narrow in the frequency space. For example, for a pumping power level that is well above the threshold of BVMSW excitation $P_p=2P_{p\,th}$ [Fig. 2(e)], the width of the frequency spectrum of the transmitted wave packet is only about 1.4% of its carrier frequency ω_s, although waves from a wide wave number range $-2\pi/L<k<2\pi/L$ take part in the parametric interaction. This small frequency width of the transmitted signal wave packet results from the inherent frequency selectivity of parametric interaction, which keeps at high amplitude level only the waves that are close to the parametric resonance surface defined by Eq. (2a).

The spectral narrowness of the parametrically interacting wave packets in the frequency space, proved by direct calculation using Eq. (6) (see Fig. 2) and retained even in the case of nonadiabatic pumping, allows us to build an approximate theory of nonadiabatic parametric interaction based on the equations for the packets' envelopes, similar to the traditional reduced equations for envelopes used in the adiabatic case [3–5,7]. However, in the nonadiabatic case we need to take into account both copropagating and contrapropagating idle wave packets simultaneously, while in the adiabatic case they were always considered separately [5,7] [see also Eqs. (3) and (4)].

To derive the generalized reduced equations for the packets' envelopes that are correct for both adiabatic and nonadiabatic pumping, we start from the model (6). For simplicity, we take only the first term in the Taylor expansion of the BVMSW dispersion law, $\omega_k=\omega_0-v|k|$, where v is the BVMSW group velocity, and assume that both $\Gamma_k=\Gamma$ and $V_{kk'}=V$ are constants calculated at the wave number k_1 (point 1 in Fig. 1). We shall denote the amplitude of all the waves propagating in the positive direction of the z axis as c_{k+} and waves propagating in the opposite direction as c_{k-}: $c_k=c_{k+}+c_{k-}$, $c_{k+}=\Theta(-k)c_k$, and $c_{k-}=\Theta(k)c_k$, where $\Theta(k)$ is the Heaviside unit function. The choice of sign in the argument of the Heaviside functions is connected with the fact that BVMSW's are backward waves, i.e., the directions of wave vector and group velocity are opposite. Making a standard Fourier transform to the z representation and retaining only the resonant terms, we get, in the approximation of spectrally narrow wave packets, the following system of reduced equations for the wave envelopes $a_+(t,z)$, $a_-(t,z)$:

$$\left(\frac{\partial}{\partial t}+v\frac{\partial}{\partial z}+\Gamma\right)a_+(t,z)=Vh_0a_-^*+Vh_{2k_1}a_+^*, \tag{10a}$$

$$\left(\frac{\partial}{\partial t}-v\frac{\partial}{\partial z}+\Gamma\right)a_-(t,z)=Vh_0a_+^*+Vh_{-2k_1}a_-^*, \tag{10b}$$

where

$$a_\pm(t,z)=\sum_{k=-\infty}^{\infty}c_{k\pm}\exp\left[i\frac{\omega_p}{2}t+i(k\pm k_1)z\right]$$

are the slowly varying envelopes of wave packets propagating in the positive ($z>0$) and negative ($z<0$) directions from the region of pumping localization. We note that the envelope amplitude $a_+(t,z)$ contains all the signal and idle partial waves propagating in the positive direction (points 1, 3, 5 in Fig. 1), while the amplitude $a_-(t,z)$ contains all the partial waves propagating in the negative direction (points 2, 4, 6 in Fig. 1). Note that group and phase velocities have opposite directions for BVMSW's. It is easy to find a transformation that converts the system (10) into a system for the amplitudes of separate partial wave packets. For example, in the case when $P_p<P_{p\,th}$ [corresponding to Fig. 2(b)] this transformation has the form

$$a_+(t,z)=a_3(t,z)\exp(-i\Delta\omega t+i\Delta kz)+a_5(t,z)\times\exp(i\Delta\omega t-i\Delta kz), \tag{11a}$$

$$a_-(t,z)=a_4(t,z)\exp(-i\Delta\omega t-i\Delta kz)+a_6(t,z)\times\exp(i\Delta\omega t+i\Delta kz), \tag{11b}$$

This transformation converts system (10) into a system of four equations describing parametric interaction of four partial wave packets: one signal and three idle wave packets corresponding to the points 3, 5, 4, and 6 in Fig. 1. Here $\Delta\omega=\omega_3-\omega_p/2$ and $\Delta k=k_3-k_1$ are the frequency and wave number detunings of the signal wave from the point $(\omega_p/2,k_1)$ on the (ω,k) plane.

The generalized system of reduced equations (10) describes the first-order parametric interaction (2) of a spectrally narrow signal with both weakly localized (adiabatic) and strongly localized (nonadiabatic) pumping, and is applicable for waves of any nature. In particular, the phenomena of pulsed signal amplification [11,13,14,16] and phase conjugation and wave front reversal [12,13,17] experimentally observed in the parametric interaction (2) of dipolar spin waves with localized electromagnetic pumping in ferrite films can be approximately described using model (10).

In the case of adiabatic weakly localized ($kL\gg1$) pumping the terms $h_{\pm2k_1}$ in Eq. (10) are vanishing, $h_{\pm2k_1}\to0$, and this system is reduced to the traditional system of envelope equations (4) that takes into account only the interaction of a signal wave packet with a contrapropagating idle wave packet [7]. On the other hand, if, as in nonlinear optics [5], the pumping is done not by a localized electromagnetic field, but by a double-frequency *wave* ($\omega_p\simeq2\omega_1, k_p\simeq2k_1$), the traditional system of reduced equations for envelope (3) can be obtained from the generalized model (10) by substituting b_{2k} for h_{2k_1} in Eq. (10a) and assuming that $h_0=h_{-2k_1}=0$ in Eqs. (10). In this case Eq. (10a) is directly reduced to Eq.

(3a) and Eq. (3b) can be obtained from it by complex conjugation. Equation (10b) is then reduced to a simple equation of a wave transfer.

It follows from the generalized model (10) that in the case of nonadiabatic pumping it is possible to realize phase conjugation and wave front reversal of optical waves in the first-order three-wave parametric process (2). So far, in optics these phenomena have been observed only in a second-order four-wave parametric interaction [18].

In the stationary regime ($\partial/\partial t=0$) the generalized system (10) can be easily solved, and, in the weakly dissipative case ($\Gamma \ll v/L$), explicit expressions for the transmitted signal power gain $K_+=P_{+out}/P_{+in}=|a_+(t,L)/a_+(t,0)|^2$ can be obtained. In the case of constructive interference between the transmitted amplified signal wave packet a_3 and the copropagating idle wave packet a_5 and $\Delta\omega\to 0$, $\Delta k\to 0$ the power gain coefficient for the transmitted signal has a maximum value K_{+max}

$$K_{+max}=\left(\cos(\kappa L)-\frac{\alpha}{\sqrt{1-\alpha^2}}\sin(\kappa L)\right)^{-2}, \qquad (12a)$$

while for the conversion coefficient $K_-=P_{-out}/P_{+in}=|a_-(t,0)/a_+(t,0)|^2$ of the input signal into the reversed signal the maximum value K_{-max} has the form

$$K_{-max}=(\sin(\kappa L)/\sqrt{1-\alpha^2})^2 K_{+max}, \qquad (12b)$$

where $\alpha=|h_{2k_1}/h_0|$ and $\kappa=h_0V\sqrt{1-\alpha^2}/v$. The expressions for the minimum amplification gain and conversion coefficients $K_{\pm min}$ in the transmitted and reversed signals are obtained from Eqs. (12) by substituting $-\alpha$ for α. In the case of adiabatic pumping ($\alpha=0$) there is no interference of wave packets, $K_{\pm max}=K_{\pm min}$, and the expressions obtained from Eqs. (12) coincide with the formulas obtained for the power amplification gain coefficients in our previous papers [12,13,19].

The threshold of BVMSW excitation by localized nonadiabatic pumping can be obtained using Eqs. (12) from the condition $K_{\pm max}\to\infty$:

$$h_{0\,th}=\frac{\arccos\alpha}{\sqrt{1-\alpha^2}}\frac{v}{LV}. \qquad (13)$$

In the adiabatic case ($\alpha=0$) Eq. (13) is reduced to the well-known expression [19] [see also Eq. (6.5.16) in Ref. [7]]

$$h_{0\,th}\simeq\frac{\pi}{2}\frac{v}{LV}. \qquad (14a)$$

In the strongly nonadiabatic case ($\alpha\to 1$) we get

$$h_{0\,th}\simeq\frac{v}{LV}. \qquad (14b)$$

It is clear that in the case of strongly nonadiabatic pumping (14b) the threshold of BVMSW excitation is $\pi/2$ times lower than in the adiabatic case (when the idle wave packet copropagating with the signal is not taken into account).

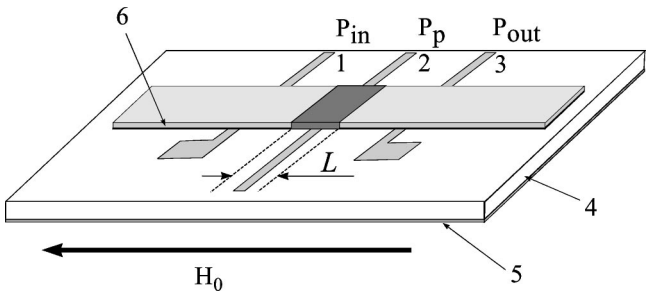

FIG. 3. Experimental setup for nonadiabatic pumping. 1, 2, and 3 are input, pumping, and output transducers, respectively; 4 is the dielectric substrate; 5 the copper screen; and 6 the YIG waveguide. Shaded area near the middle transducer shows the pumping localization region of length L.

The modulation coefficient (9) in both transmitted and reversed waves turns out to be the same, and is defined by the expression

$$K_{mod}=\frac{2\alpha\sqrt{1-\alpha^2}\sin(\kappa L)\cos(\kappa L)}{(1-\alpha^2)\cos^2(\kappa L)+\alpha^2\sin^2(\kappa L)}. \qquad (15)$$

Obviously, in the adiabatic case ($\alpha=0$) the modulation coefficient (15) vanishes. In the nonadiabatic case for relatively small pumping amplitudes ($h_0\ll h_{0\,th}$) the modulation coefficient increases linearly with increase in the pumping amplitude,

$$K_{mod}\simeq 2\alpha h_0 LV/v. \qquad (16a)$$

In the strongly nonadiabatic case ($\alpha\to 1$) the modulation coefficient approaches unity when the pumping amplitude approaches the threshold of BVMSW generation (14b):

$$K_{mod}\simeq\frac{2h_0/h_{0\,th}}{1+(h_0/h_{0\,th})^2}. \qquad (16b)$$

Experimental investigations of the interaction of a spectrally narrow wave packet with nonadiabatic parametric pumping were performed on dipolar spin waves, namely, backward volume magnetostatic waves, propagating in a high-quality yttrium iron garnet (YIG) film. We chose BVMSW's for these experiment because it is relatively easy to create nonadiabatic ($L<\lambda$) pumping conditions for these waves.

Our experimental structure is shown in Fig. 3. It consists of three thin silver wires (diameter $d=30$ μm) that play the roles of input 1, pumping 2, and output 3 transducers and were in direct contact with an YIG waveguide, i.e., a rectangular sample of an YIG film epitaxially grown on a gallium gadolinium garnet substrate. The thickness of the YIG waveguide was 4.9 μm, while the in-plane sizes were 1.6 mm $\times$18 mm. The YIG waveguide was oriented in such a way that its short side was parallel to the wires. The three silver wire transducers were situated on a free surface of a screened dielectric (Al_2O_3) plate of thickness 0.5 mm at a distance 3.75 mm from each other, so that the signal wave propagation length from the input to output transducer was 7.5 mm.

The YIG waveguide in the structure described above was magnetized to saturation ($4\pi M_0 = 1750$ Oe) by the in-plane constant bias magnetic field $H_0 = 1015$ Oe oriented perpendicularly to the wire transducers. In such a geometry the input transducer 1 can effectively excite BVMSW's propagating mostly perpendicular to the transducer and having wave numbers $|k| < \pi/d$.

The middle 2 transducer played the role of a pumping source that created in the YIG film a region of localized (nonpropagating with $k_{p0} = 0$) microwave magnetic field $\mathbf{h}_p$ that was mostly parallel to the bias field $\mathbf{H}_0$. The pumping frequency supplied to the transducer 2 was two times larger than the frequency of the signal supplied to the input transducer: $\omega_p = 2\omega_s = 2\pi \times 9446$ MHz. The BVMSW wave number corresponding to the pumping frequency ω_p was substantially larger than π/d, and, therefore, the pumping transducer could not linearly excite a propagating BVMSW at the frequency ω_p. The pumping transducer 2 was made as a half-wavelength open microstrip resonator tuned to the pumping frequency ω_p, and having a loaded Q factor of $Q = 20$. When a pumping electromagnetic signal of frequency $\omega_p = 2\omega_s$ was supplied to this resonator, a region of pumping magnetic field localization was created around it. The effective length L of this region in the direction of the signal wave propagation is determined mostly by the wire diameter d, but also by the thickness and dielectric permeability of the dielectric substrate, and is of the order of several wire diameters d. The value of the pumping localization length L, in the case when the group velocity of the signal wave is known, can be evaluated experimentally by measuring the time dependence of the influence of the pulsed pumping on the linear signal transmitted through the pumping localization region (for details see Ref. [13]). For our experimental structure (Fig. 3) it was experimentally evaluated as $L = 0.1$ mm.

The magnitude of the bias magnetic field $H_0 = 1015$ Oe in our experiments was chosen in such a way that the carrier wave number k_1 of the signal wave packet was $k_1 = 100$ cm^{-1} when the signal carrier frequency was exactly half of the central pumping frequency $\omega_s = \omega_p/2 = 2\pi \times 4723$ MHz. It is clear that for these parameters our pumping was nonadiabatic, as $k_1 L \simeq 1$.

The other measured parameters of our experiments are the group velocity at the signal carrier frequency $v = -2.24$ cm/μs; the signal propagation time from the input to output transducer $t_{prop} = 334$ ns; the ferromagnetic resonance linewidth of the YIG film sample $2\Delta H = 0.4$ Oe; the signal pulse duration $\tau_s = 20$ ns; the signal input power $P_s \leqslant 5$ mW; the pumping pulse duration $\tau_p = 30$ ns; the pumping power $0 \leqslant P_p \leqslant 5$ W; and the threshold pumping power at which generation of half-frequency BVMSW's took place, $P_{p\,th} = 3.9$ W.

The experimentally measured resonance ($\omega_s = \omega_p/2$) values of the power gain coefficient for the transmitted signal wave packet $K_+ = P_{+out}/P_{+in}$ and for the conversion coefficient into the reversed wave packet $K_- = P_{-out}/P_{+in}$ as functions of the pumping power P_p are presented in Fig. 4 and Fig. 5, respectively. The measurements were made in the pulsed regime using signal and pumping microwave generators that have random initial phases. Thus, the phase difference between the signal and pumping at the moment of their interaction in the pumping localization region was arbitrary, and different for each repetition of this interaction. Therefore, the power gain coefficients for the transmitted K_+ and reversed K_- wave packets, as well as their amplitudes $A_\pm$, were changing from maximum ($K_{\pm max}$, $A_{\pm max}$) to minimum ($K_{\pm min}$, $A_{\pm min}$) values depending on this randomly changing phase, i.e., random modulation of the amplified transmitted and reversed signals was observed.

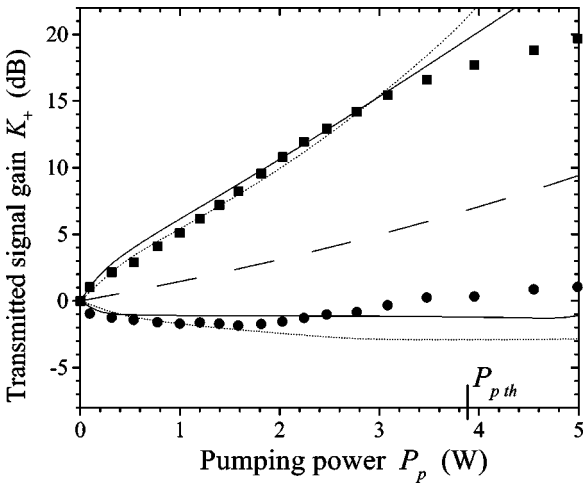

FIG. 4. Maximum and minimum power gain coefficients for the signal wave packet transmitted through the region of pumping localization in the case of nonadiabatic pumping: squares and circles show the experimental values of K_{+max} and K_{+min}, respectively; solid lines are calculated from the model (6); dotted lines are calculated from the approximate model (10); broken line in the middle is calculated from the model (4) for adiabatic pumping.

The experimental values of $K_{\pm max}$ are shown in Fig. 4 and Fig. 5 by squares, while the experimental values of

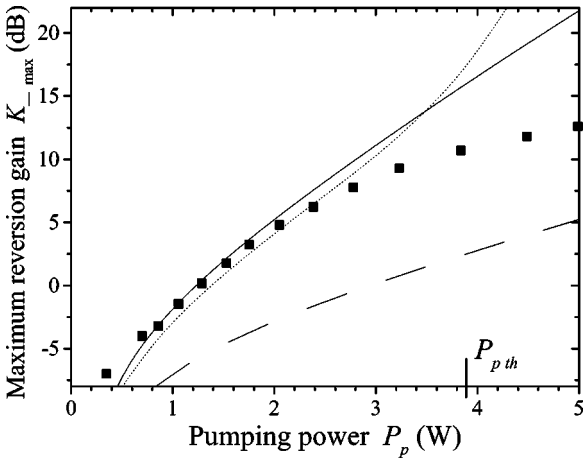

FIG. 5. Maximum power conversion coefficients for the wave packet reversed from the region of pumping localization in the case of nonadiabatic pumping: squares show the experimental values of K_{-max}; solid line is calculated from the model (6); dotted line is calculated from the approximate model (10); broken line is calculated from the model (4) for adiabatic pumping.

K_{+min} are shown in Fig. 4 by circles. The solid lines in Figs. 4 and 5 show the results of direct numerical calculation using the model (6) when 300 waves having wave numbers in the interval from $-300\ \mathrm{cm}^{-1}$ to $+300\ \mathrm{cm}^{-1}$ were taken into account. The dotted lines in Figs. 4 and 5 show the results obtained using the approximate generalized envelope equations (10). The broken line in the center shows the results obtained from the traditional envelope equations derived for the case of adiabatic pumping [5,7] [or obtained from Eq. (10) for $h_{\pm 2k_1} \rightarrow 0$].

It can be clearly seen that for moderate pumping powers the generalized envelope equations (10) derived in this paper give a good quantitative description of the experiment, and do not differ much from the results of direct numerical simulation in *k* space performed using the model (6). On the other hand, the traditional envelope equations, obtained for adiabatic pumping, give results that have nothing to do with reality, and do not describe the experiment even qualitatively.

With increasing pumping power the experimental results begin to differ significantly from the results of calculations. These differences may be caused by parametric excitation of plane spin waves at high pumping powers [9,13]. The appearance of these plane spin waves reduces the influence of phase differences between the signal and pumping, and, consequently, leads to a decrease of $K_{\pm max}$ and an increase of $K_{\pm min}$.

Figure 6 shows the modulation coefficient of the transmitted signal [see Eq. (9)] as a function of the relative amplitude of the pumping magnetic field (or supercriticality) h_0/h_{0th}. This scale on the horizontal axis was chosen to conveniently compare the experiment with the approximate theoretical expression (16b). It can be clearly seen that the experimental modulation coefficient increases linearly with h_0 for relatively low values of the pumping amplitude, and saturates at unity for values of supercriticality close to 1, in good agreement with the theoretical prediction (16b). It is also clear from Fig. 6 that the results of calculations obtained from the approximate generalized system of reduced envelope equations (10) are in good agreement with both the experimental results and the results of direct numerical modeling using Eq. (6).

In conclusion, the interaction of a spectrally narrow propagating wave packet with nonadiabatic parametric pumping localized in a region of size the order of the carrier signal wavelength ($L \sim \lambda$) was investigated theoretically and experimentally. A system of generalized reduced equations for the envelopes of interacting wave packets was derived and successfully used to describe the experimental results in the case of nonadiabatic parametric pumping.

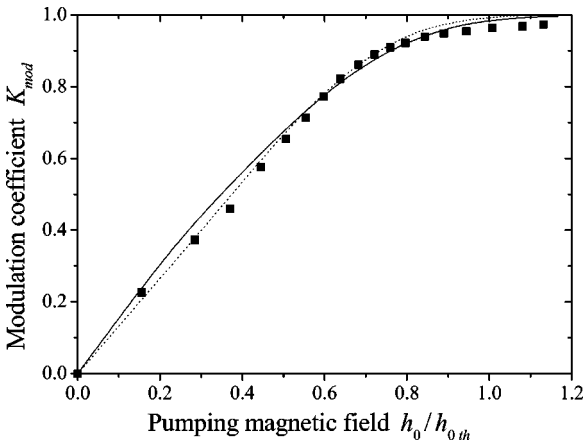

FIG. 6. Modulation coefficient of the output signal for different values of pumping supercriticality: squares, experiment; solid line, calculation from the model (6); dotted line, calculation from the approximate model (10).

The unusual feature of nonadiabatic three-wave parametric interaction of the first order is the simultaneous excitation of idle wave packets that are both copropagating and contrapropagating with the transmitted signal wave packet. This property of nonadiabatic three-wave parametric interaction opens the possibility of observing wave front reversal and phase conjugation of optical waves in the first-order three-wave parametric process (2). To the best of our knowledge these phenomena in nonlinear optics have so far been observed only in second-order four-wave parametric processes [18].

This work was partially supported by the U.S. Civilian Research and Development Foundation (Grant No. UP1-2120), by the U.S. National Science Foundation (Grant No. DMR-0072017), and by the Oakland University Foundation.

[1] L. D. Landau and E. M. Lifshitz, *Course of Theoretical Physics, Vol. 2: Field Theory* (Pergamon, Oxford, 1966).
[2] V.S. L'vov and A.M. Rubenchik, Zh. Éksp. Teor. Fiz. **72**, 127 (1977) [Sov. Phys. JETP **45**, 67 (1977)].
[3] J.A. Armstrong, N. Bloembergen, J. Ducuing, and P.S. Pershan, Phys. Rev. **127**, 1918 (1962).
[4] Y. R. Shen, *The Principles of Nonlinear Optics* (J. Wiley and Sons, Inc., New York, 1984).
[5] N. Bloembergen, *Nonlinear Optics* (Benjamin, Reading, MA, 1977).
[6] V.E. Zakharov, Zh. Éksp. Teor. Fiz. **62**, 1745 (1972) [Sov. Phys. JETP **35**, 908 (1972)].
[7] V. S. L'vov, *Wave Turbulence Under Parametric Excitation* (Springer, Berlin, 1994).
[8] L.M. Gorbunov, Zh. Éksp. Teor. Fiz. **67**, 1386 (1974) [Sov. Phys. JETP **40**, 689 (1974)].
[9] A. G. Gurevich and G. A. Melkov, *Magnetization Oscillations and Waves* (CRC Press, New York, 1996).
[10] R.W. Damon and J.R. Eshbach, J. Phys. Chem. Solids **19**, 308 (1961).
[11] A.V. Bagada, G.A. Melkov, A.A. Serga, and A.N. Slavin, Phys. Rev. Lett. **79**, 2137 (1997).
[12] A.L. Gordon *et al.*, Pis'ma Zh. Éksp. Teor. Fiz. **67**, 869 (1998) [JETP Lett. **67**, 913 (1998)].
[13] G.A. Melkov *et al.*, Zh. Éksp. Teor. Fiz. JETP **89**, 1189 (1999).

[14] B.A. Kalinikos *et al.*, Pis'ma Zh. Éksp. Teor. Fiz. **66**, 346 (1997) [JETP Lett. **66**, 371 (1997)].
[15] W. H. Louissel, *Coupled Mode and Parametric Electronics* (J. Wiley and Sons, Inc., New York, 1960).
[16] B.A. Kalinikos and M.P. Kostylev, IEEE Trans. Magn. **33**, 3445 (1997).
[17] G.A. Melkov *et al.*, Phys. Rev. Lett. **84**, 3438 (2000).
[18] B. Ya. Zel'dovich, N. F. Pilipetsky, and V. V. Shkunov, *Principles of Phase Conjugation* (Springer, Berlin, 1985).
[19] G.A. Melkov and S.V. Sholom, Zh. Éksp. Teor. Fiz. **60**, 118 (1990) Sov. Phys. Tech. Phys. **35**, 943 (1990).